

Master's thesis
Master's programme in Atmospheric Sciences
Aerosol Physics

Verification of the Carbonaceous Aerosol Speciation System (CASS) with offline filter measurements in Hyytiälä 2023

J. Tapio Elomaa
07.09.2026

Supervisor(s): PhD. Krista Luoma, Prof. Tuukka Petäjä
Examiner(s): Prof. Katrianne Lehtipalo, Prof. Tuukka Petäjä

UNIVERSITY OF HELSINKI
FACULTY OF SCIENCE
PL 64 (Gustaf Hällströmin katu 2a)
00014 Helsingin yliopisto

Faculty – Tiedekunta – Fakultet	Degree programme – Koulutusohjelma – Utbildningsprogram	
Faculty of Science	Master's programme in Atmospheric Sciences Aerosol Physics	
Author – Tekijä – Författare		
J. Tapio Elomaa		
Title – Työn nimi – Arbetets title		
Verification of the carbonaceous aerosol speciation system (CASS) with offline filter measurements in Hyytiälä		
Level – Työn laji – Arbetets art	Month and year – Aika – Datum	Number of pages – Sivumäärä – Sidantal
Master's thesis	07/09/2026	34

Abstract – Tiivistelmä – Referat

Carbonaceous aerosol (CA) particles constitute a major fraction of atmospheric fine particulate matter (PM). CA particles have complex compositional and optical properties affecting climate directly through absorption and scattering of solar radiation and indirectly though cloud interaction and have negative health effects on humans. Currently the scientific community has *low confidence* in the distribution and effects of individual CA components to the climate due to the lack of observational data.

The aim of this thesis is to characterize the performance of the Carbonaceous Aerosol Speciation System (CASS) in comparison to traditional filter measurements analysed with the Lab OC/EC Aerosol Analyzer in a boreal forest environment. The measurements were conducted at SMEAR II in Hyytiälä, Finland, during 11/2022-09/2023. The CASS system is designed to provide semi-automatic and resource efficient method to potentially increase the measurement coverage of CA components. The candidate system showed good correlation (~0.9) for organic, black and total carbon compared to the reference. The system was better at capturing low concentrations and it measured at higher time resolution than the reference. Optically determined black carbon in the CASS and its equivalent thermally determined elemental carbon showed multiple sources of uncertainty. For the accurate measurement and determination of these fractions' additional studies on the thermal-optical properties of carbonaceous aerosol are needed. Compared to a previous study conducted in 2007, the annual concentration of carbonaceous aerosol reduced in Hyytiälä by 45% for organic carbon and 66% for elemental/black carbon. Seasonally summertime organic carbon remained the same, but annual elemental/black carbon and wintertime organic carbon showed significant reduction.

Keywords – Avainsanat – Nyckelord

Organic Carbon, Elemental Carbon, Black Carbon, Carbonaceous Aerosol Speciation System, Thermal-Optical Measurement Methods

Where deposited – Säilytyspaikka – Förvaringsställe

Additional information – Muita tietoja – Övriga uppgifter

Table of contents

1 Introduction 1

2 Methods 3

2.1 Measurement site 3
2.2 Instruments 3
2.2.1 Filter collection and analysis with Lab OC/EC Aerosol Analyzer 3
2.2.2 Carbonaceous Aerosol Specification System (CASS) 7
2.3 Data processing and error estimation 10
2.3.1 Lab OC/EC error estimation 10
2.3.2 CASS system error estimation 11
2.3.3 Aethalometer scattering correction 11
2.3.4 Data processing and tools 12

3 Results 13

3.1 Annual and seasonal concentrations of carbonaceous aerosol at SMEAR II 13
3.2 Correlation between filter and CASS measurements 15
3.3 Seasonal correlation between filter and CASS measurements 18
3.4 Ratio of organic and elemental carbon and the evolution of mass absorption cross section 19

4 Conclusions 23

5 References 25

Nomenclature

Symbol	Description	Unit
A	Area	m^2
AAE	Absorption Ångström exponent	
ACTRIS	The Aerosol, Clouds and Trace Gases Research Infrastructure	
A_p	Area of a filter punch	
ATN	Attenuation	
BC	Black Carbon	
BrC	Brown Carbon	$\mu g\ m^{-3}$
CA	Carbonaceous aerosol particles	
CABM	Canadian Aerosol Baseline Measurement	
CASS	Carbonaceous Aerosol Speciation System	
CC	Carbonate Carbon	$C\ \mu g\ m^{-3}$
C_{ref}	Multiple scattering parameter	
eBC	Equivalent Black Carbon, i.e., optically determined black carbon concentration	$\mu g\ m^{-3}$
EC	Elemental Carbon	$C\ \mu g\ m^{-3}$
ECT9	EnCan-Total-900 Thermal protocol	
eEC	Equivalent Elemental Carbon, i.e., optically determined elemental carbon concentration	$\mu g\ m^{-3}$
eOC	Equivalent Organic Carbon, i.e., optically determined organic carbon concentration	$\mu g\ m^{-3}$
f	Loading correction	
FID	Flame Ionization Detector	
GAW	Global Atmospheric Watch	
H	Harmonization factor	
I	Intensity through a filter	$W\ m^{-2}$
I_0	Intensity through a reference	$W\ m^{-2}$
IC	Inorganic Carbon	$C\ \mu g\ m^{-3}$
ICOS	Integrated Carbon Observation System	
IMPROVE	Interagency Monitoring of Protected Visual Environments	
IMPROVE_A	Thermal protocol	

IPCC	Intergovernmental Panel on Climate Change	
LAC	Light Absorbing Carbon	
MAAP	Multi Angle Absorption Photometer	
MAC	Mass Absorption cross-section	$m^2\ g^{-1}$
NDIR	Nondispersive infrared sensor	
NIOSH	Thermal protocol developed and named after the National Institute for Occupational Safety & Health (USA)	
OC	Organic Carbon	C $\mu g\ m^{-3}$
OM	Organic Matter	
PC	Pyrolytic Carbon	C $\mu g\ m^{-3}$
PM	Particulate Matter (cut offs marked with subscripts 1 µm, PM_1, $PM_{2.5}$, PM_{10})	
Q	Volumetric flow rate	$l\ min^{-1}$
s	Aerosol scattering correction factor	
SAE	Scattering Ångström exponent	
SMEAR	Station for Measuring Ecosystem-Atmosphere Relations	
SOP	Standard Operating Procedure	
TC	Total Carbon	C $\mu g\ m^{-3}$
TCA	Total Carbon Analyzer	
TOA	Thermal Optical Analysis	
TOR	Thermal-Optical Reflectivity -method	
TOT	Thermal-Optical Transmission -method	
V	Volume	
WMO	World Meteorological Organization	
σ_{abs}	Absorption coefficient	Mm^{-1}
σ_{ATN}	Attenuation coefficient	Mm^{-1}
σ_{BLANK}	Standard deviation of the fieldblanks	
σ_{scat}	Scattering coefficient	Mm^{-1}

1 Introduction

Carbonaceous aerosol (CA) particles constitute a major fraction of atmospheric fine particulate matter (PM). CA particles have complex compositional and optical properties affecting climate directly through absorption and scattering of solar radiation and indirectly though cloud interaction (Jimenez et al., 2009; IPCC, 2021). In addition, PM has been shown to have negative health effects (Pope & Dockery, 2006; Janssen et al., 2011; Shiraiwa et al., 2017; Arfin et al., 2023). CA can be defined with several terms. These include organic carbon (OC or eOC), organic matter (OM), elemental carbon (EC), inorganic or carbonate carbon (IC, CC), total carbon (TC), black carbon (BC or eBC), brown carbon (BrC) and generally light absorbing carbon (LAC). The variety of terms and abbreviations are commonly used due to differing definitional and measurement method dependent reasons. Prefix *e*, which stands for *equivalent*, denotes that an optical measurement method is used (Petzold et al., 2013; Monteiro dos Santos et al., 2016; Rovira et al., 2025).

Organic matter approximately accounts for 20-90 % of PM under 2.5 μm in diameter ($PM_{2.5}$) (Jimenez et al., 2009) and overall CA account 50-70% of PM under 1 μm in diameter (PM_1) (IPCC, 2021). The emission of CA particles comes both from primary and secondary sources. These sources are mainly biomass and fossil fuel combustion, and natural emissions of precursor gases. In the atmosphere the particles and gases are influenced by a variety of complex physical and chemical processes affecting the formation, size, growth, composition and optical properties of the particles. Overall CA have a cooling effect on the climate though direct scattering and cloud interactions, but local warming due to absorption from BC. The IPCC (2021) report states *low confidence* in the distribution and effects of individual CA components to the climate due to the lack of observational data.

Therefore, a new Carbonaceous Aerosol Speciation System (CASS) is developed by Magee Scientific (Magee, 2026) combining a thermal total carbon analyser (TCA08) with an optical Aethalometer (AE36) in order to determine the TC, eOC, eBC and eBrC concentration in the atmosphere (Rigler et al., 2020). This system is aimed to provide a relatively low-cost solution to increasing the observational data of CA. Even though the system does not provide information of individual CA compounds, it offers an option to

measuring the overall trends of the definitional groups. This could be utilized to improve the estimation and modelling of the effect CA have on the climate.

The aim of this thesis is to characterize the performance of the Carbonaceous Aerosol Speciation System (CASS) in comparison to filter measurements analysed with the Lab OC/EC Aerosol Analyzer in a boreal forest environment. Lab OC/EC Aerosol Analyzer is commonly used reference method for OC/EC concentrations (Karanasiou et al., 2015). The measurements were conducted in Hyytiälä, Finland, during 11/2022-09/2023. The focus of this study is on the connection between aerosol absorption and OC/EC/TC mass concentrations and their evolution over time. The use of different thermal-optical methods for measuring carbonaceous aerosols is demonstrated and discussed.

2 Methods

This section describes the measurement location, the methods and instruments used in the data collection, analysis and error estimation procedures used in this thesis.

2.1 Measurement site

Station for Measuring Ecosystem-Atmosphere Relations (SMEAR) II (Hari & Kulmala, 2005; Neefjes et al., 2022) is a boreal forest background station designed to study atmospheric, soil and forest sciences. The station is located in Hyytiälä, southern Finland (61°51´N, 24°17´E, 181 m above sea level). The surroundings consist of homogenous Scots pine (*Pinus sylvestris*) forest with a small lake approximately 1 km from the station. The nearest major population centers are Tampere (~255 000) and Jyväskylä (~147 000) about 60 and 100 km away respectively. Otherwise, the location is sparsely populated. The station is part of the Aerosol, Clouds and Trace Gases Research Infrastructure (ACTRIS, Laj et al., 2024) and Integrated Carbon Observation System (ICOS, Heiskanen et al., 2022) infrastructure networks.

2.2 Instruments

2.2.1 Filter collection and analysis with Lab OC/EC Aerosol Analyzer

Filters were collected between 28.11.2022 and 25.9.2023. The filter collection was done on Pallflex Tissuequartz 2500-QAT-UP quartz fiber filters with a flow rate of 39 liters per minute (lpm) and a collection time on average 2-3 days. The sample was collected from approximately 8 m above the ground, but inside the forest canopy. The diameter of the filter is 47 mm, and the diameter of the collection area is 35 mm. The inlet system utilized a PM10 impactor cutting off particles larger than 10 μm in diameter. After collecting the filters were stored in a freezer and transported to Helsinki in a cooled container for analysis with a Lab OC/EC Aerosol Analyzer.

Lab OC/EC aerosol analyzer M5L developed by Sunset Laboratory Inc. (Tigard, OR, USA) is an instrument utilizing a thermal optical analysis (TOA) method to determine OC/EC mass concentrations (Huntzicker J. J. and Johnson, 1982; Birch & Cary, 1996; Watson et al., 2005; Lack et al., 2014). CA collected on a quartz fiber filter are thermally desorbed and combusted by heating the filter material in controlled steps within a sample oven. The CA turns into methane, which is measured with a flame ionization detector

(FID). The instrument design can be seen in Fig. 1. and an example of the heating "protocol" can be seen in a thermogram in Fig. 2.

A rectangular filter punch of 1.5 cm^2 was cut from the original filter and placed into the oven. The temperature was then raised to approximately 850–900 °C in an inert environment of pure helium (He). The more volatile OC and carbonate carbon (CC) desorbs from the filter fiber and is guided into an oxidizer, where the molecules of carbon are catalytically converted to CO_2 with manganese-dioxide (MnO_2). The CO_2 is further converted into methane with hydrogen (H_2) and a nickel (Ni) catalyst in a methanator. The resulting methane concentration is measured with the FID. During the heating process up to 30% of the OC can pyrolyze into pyrolytic carbon (PC). PC is more stable than OC and will only combust in an oxygenated (O_2) environment. Therefore, PC will affect the second measurement phase and the EC measurement (Sunset Labs, 2024).

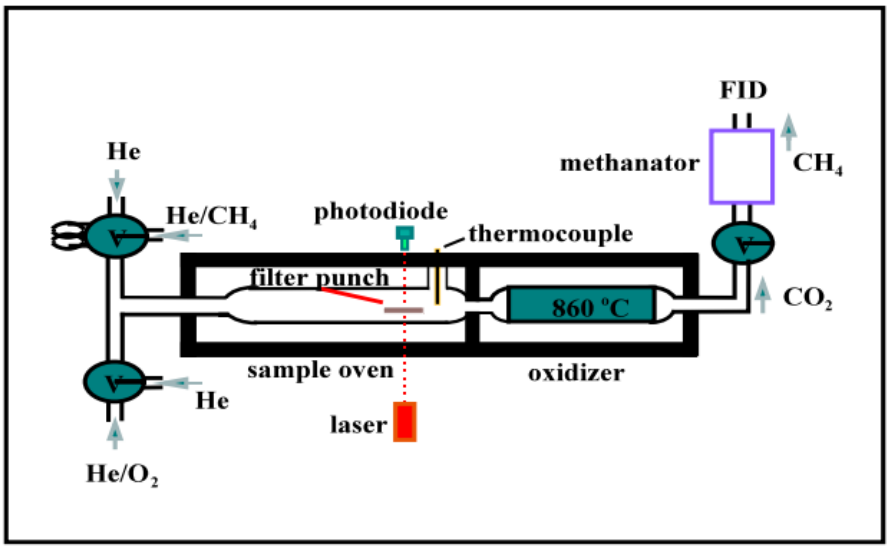


Figure 1. Schematic of the Lab OC/EC aerosol analyzer. Copied from NIOSH Manual of Analytical methods 4th edition, Chapter Q, Fig. 1 (NIOSH, 2003).

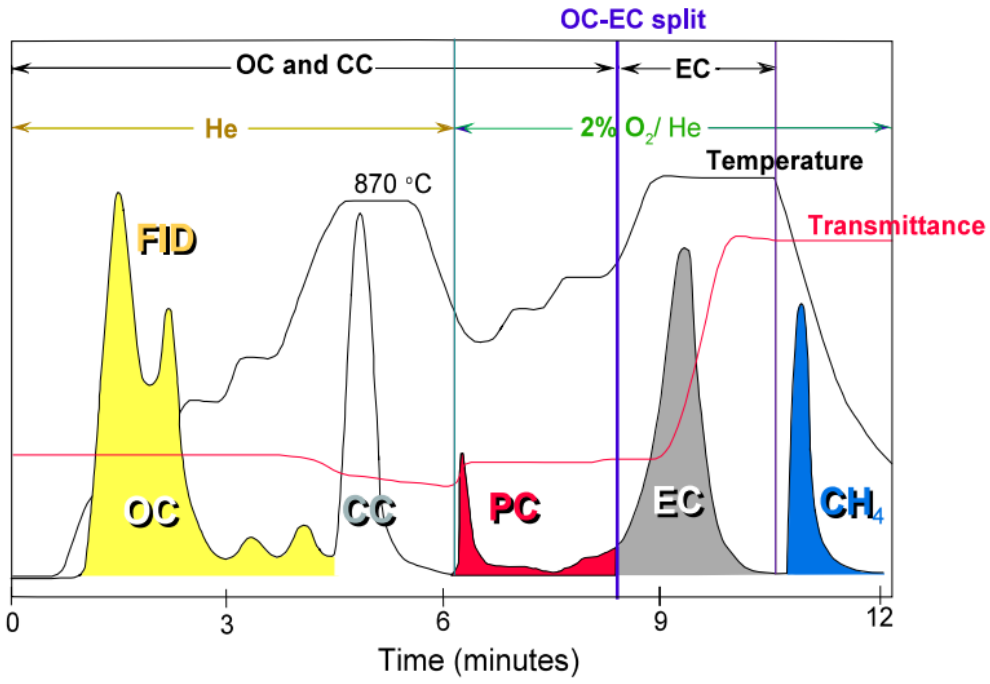


Figure 2. Example thermogram of a TOA instrument. The sample contains organic carbon (OC), carbonate carbon (CC), pyrolytic carbon (PC) which is formed from OC pyrolyzing into PC due to heating, and elemental carbon (EC). Last spike is methane calibration peak. Copied from NIOSH Manual of Analytical methods 4th edition, Chapter Q, Fig. 2 (NIOSH, 2003).

In the second measurement phase the gas is changed to 2% O_2/He mixture, and the PC and EC will combust forming CO_2, which is similarly converted to methane and the concentration measured with the FID. To correct for the PCs effect on the EC measurement, the optical part of the instrument is applied with a so-called thermal-optical transmittance (TOT) -method. In the method an optical laser (660 nm) is used to measure the transmittance of the filter punch. During the formation of the PC the filter will get darker, lowering the transmittance of the filter as seen with the red line in Fig. 2. Therefore, a cut-off point is created when the transmission reaches back to the original value, marked as the blue vertical line in Fig. 2. The concentration before the cut-off point is considered OC and after the cut-off point EC. Finally, with each measurement the instrument calibrates automatically by measuring a known amount of methane to ensure proper operation.

Before every measurement day zero and a sucrose sample is analyzed to ensure the correct calibration of the instrument. The detection limit of the instrument is 0.2 µg cm^{-2} and the

precision 4–6%, when the OC concentrations are between 5–400 μg cm^{-2} and EC concentrations 1–15 μg cm^{-2}, respectively.

2.2.1.1 TOA Method errors, i.e., Protocols and optical corrections

With the TOA methods there can be a large difference in the OC/EC determination depending on the thermal protocol and the optical correction method used in the measurement. Therefore, the thermal protocol and optical correction method needs to be reported with the measurements and the choice of thermal protocol needs to considered in comparisons. The most common thermal protocols used have been the NIOSH (Chow et al., 2001), IMPROVE_A (Chow et al., 2007) and EUSAAR-2 (Cavalli et al., 2010). Also, a purely thermal analysis method EnCan-total-900 (ECT9) has been used (Huang et al., 2006; Chan et al., 2019). IMPROVE_A is the standard operation procedure (SOP) used in the Interagency Monitoring of Protected Visual Enviroments (IMPROVE) network and other networks in USA. IMPROVE_A is an advancement to the older NIOSH protocol. EUSAAR-2 is the SOP used in Europe within the ACTRIS network. ECT9 is used by Canadian Aerosol Baseline Measurement Program (CABM). Further complications are caused as the optical method for correcting the PC can be implemented either by measuring the transmittance thought the filter as described before with the TOT method or by measuring the reflectance of the filter with the thermal-optical reflectance (TOR) method.

Differences between the thermal protocols have previously been reported between the NIOSH TOT and IMPROVE TOR, where NIOSH have been found to report less than half of the EC concentrations (Chow et al., 2001). This is attributed to the TOT corrected measurements for EC being lower than TOR corrected measurements by up to 30% when using the same thermal protocol and up to 70–80% lower for NIOSH when compared to IMPROVE_A (Chow et al., 2004) (Vice versa $OC_{TOT} > OC_{TOR}$). In addition, the composition of the aerosol affects the measurement with differences between locations reported that the EC_{TOT} was 50% lower than EC_{TOR} at rural sites and 20% lower at urban sites (Chiappini et al., 2014) (Vice versa $OC_{TOT} > OC_{TOR}$). In a study comparing NIOSH, IMPROVE_A and EUSAAR-2, for EC, NIOSH was found to have a negative bias due to premature combustion of EC, IMPROVE_A positive bias due to too low temperature to desorb all the OC and EUSAAR-2 showing most accuracy with its design minimizing these effects. Still a slightly modified IMPROVE_A was found to be the best solution for the application due to the protocol adjusting the heating times to be so long that the FID

reaches baseline level before moving to the next heating step (Bautista et al., 2015). Finally, ETC9 has been found to report TC, OC, and EC values higher than 20–30%, 0–15% and 60–80% respectively when compared to the IMPROVE_A TOR (Chan et al., 2019).

The Global Atmospheric Watch (GAW) programme of the World Meteorological Organization (WMO) accepts data with any thermal protocol with clear descriptions, but recommends the use of IMPROVE_A, EUSAAR-2 and ETC9. For this study the highest relevance is to note that the difference between TC measurements is relatively small between the thermal protocols.

2.2.2 Carbonaceous Aerosol Specification System (CASS)

Carbonaceous Aerosol Specification System (CASS, Aerosol d.o.o., Slovenia, EU), is an instrument system composed of a Total Carbon Analyzer TCA08 and an Aethalometer AE33 or AE36 measuring TC and eBC respectively. In the system eBC is assumed to be the optically equivalent parameter to EC. The system calculates eOC with a simple subtraction of eBC from the TC. The CASS system was run with $PM_{2.5}$ inlet.

2.2.2.1 Total Carbon Analyzer (TCA08)

The total carbon analyzer (TCA08) is an instrument utilizing a thermal method of determining the TC concentration of a collected sample (Rigler et al., 2020). The instrument consists of two parallel burners that alternate between collection and analysis. In both burners the sample is collected to a 47 mm diameter quartz fiber filter on a 4.9 cm^2 collection spot with a flow rate of 16.7 lpm. After collection the flow is changed from one burner to the other for collection. The analyzing burner changes to a reduced analytic flow rate of 0.5 lpm. During the analysis the CA is combusted in a filtered air environment by heating the burner up to 940 °C almost instantly. CA combusts into CO_2, which is measured with a non-dispersive infrared (NDIR) gas analyzer. The analytic air is pumped though a 10 L buffer volume to ensure that the CO_2 concentration of the air is stable during the analysis. The analysis takes approximately 20 minutes and therefore the collection time of the instrument can be set between 20 minutes to 24 hours. The use of two burners gives the instrument the ability to make continuous measurements with a high time resolution. Also, the use of filtered air makes it easier to deploy the instrument for in-situ measurements as it does not rely on external gas mixtures. The quartz filters

can be used in multiple burns and during the measurements they were changed every 2–3 weeks.

The measurement method can have positive and negative artifacts mainly due to organic gases adsorbing into the quartz filter fibers causing overestimation of the TC concentration and volatilization of the collected aerosol causing underestimation of the TC respectively. In the measurement setup the positive artifact was taken into account by using a charcoal denuder in the inlet line. The denuder efficiently (~70-80 %) removes organic gases from the sample flow via diffusing the gases to the denuder surfaces. The efficiency of the denuder reduces overtime as the surfaces get saturated. The denuders were tested every 6 months during the measurements with efficiency of 73% in 27.04.2023 and 81% in 04.01.2024. The volatization effects are considered to be small as the filters are not handled in the CASS system (Rigler et al., 2020).

2.2.2.2 AE36s Aethalometer

An aethalometer is an instrument utilizing an optical method to measure the absorption coefficient of aerosol particles and deriving the equivalent black carbon (*eBC)* concentration from it. The instrument design of the AE36s Aethalometer (Magee Scientific Aerosol d.o.o., Slovenia, EU) can be seen in Fig. 3.

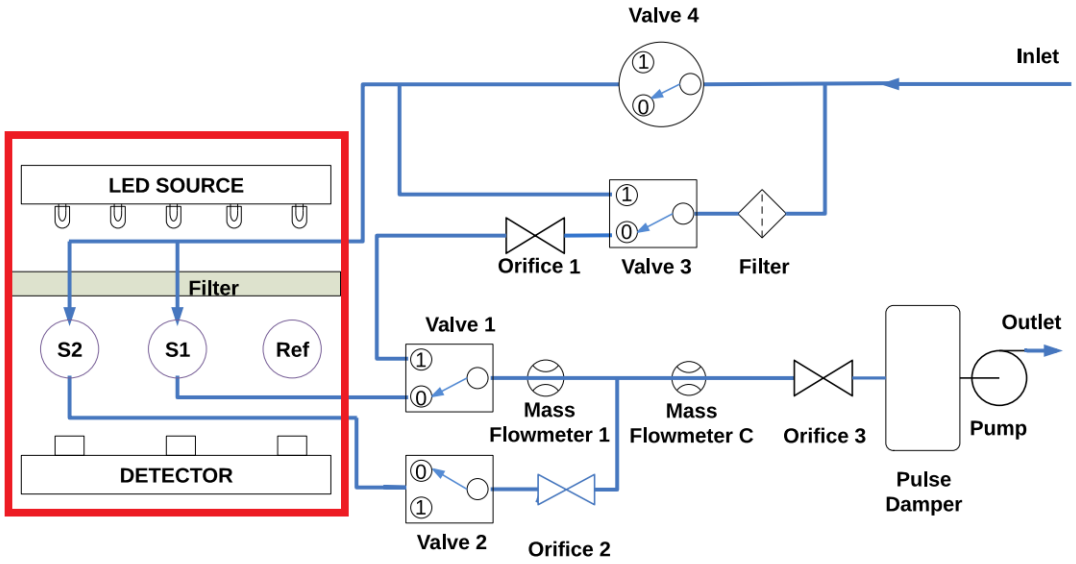


Figure 3. Schematic of the Aethalometer. The red box marks the optical chamber where the measurement is made. (Edited Fig. 1 from Drinovec et al. (2015)*)*

In the measurement method aerosol particles are collected on a quartz filter and the attenuation of light through the filter is measured as

$$ATN = 100 * ln\left(\frac{I_0}{I}\right), \quad [1]$$

where I is the intensity through the filter and I_0 is the intensity through a reference filter. The change in attenuation overtime is directly related to the collected aerosol as

$$\sigma_{ATN} = \frac{dATN}{dt} * \frac{A}{Q}, \quad [2]$$

where σ_{ATN} is the attenuation coefficient, A is the filter area and Q is the volumetric flow rate through the filter. The attenuation consists of absorption and scattering from the aerosol, scattering from the filter fibers and the non-linearity response of the accumulation of particles. To determine the absorption coefficient, these artifacts need to be corrected from the attenuation coefficient as

$$\sigma_{\text{abs}} = \frac{f * \sigma_{ATN} - s * \sigma_{\text{scat}}}{C_{\text{ref}}}, \quad [3]$$

where σ_{abs} is the absorption coefficient, f is the loading correction for the non-linearity response, s is a fraction of the scattering coefficient σ_{scat} of the aerosol particles and C_{ref} is a constant accounting the multiple scattering between the filter fibers and aerosol particles (Virkkula et al., 2015). The σ_{abs} can be used to determine the eBC concentration with a mass absorption cross-section (MAC, 370 nm - 18.47 $m^2\ g^{-1}$, 470 nm - 14.54 $m^2\ g^{-1}$, 520 nm - 13.14 $m^2\ g^{-1}$, 590 nm - 11.58 $m^2\ g^{-1}$, 660 nm - 10.35 $m^2\ g^{-1}$, 880 nm - 7.77 $m^2\ g^{-1}$, 950 nm - 7.19 $m^2\ g^{-1}$) described as seen in Eq. 4.

$$EC \sim eBC = \frac{\sigma_{abs}}{MAC} \quad [4]$$

An AE33 Aethalometer uses 7 wavelengths (370, 470, 520, 590, 660, 880 and 950 nm) to measure the σ_{abs}. The prototype model AE36s used in this study has additional 2 wavelengths (340 nm, 400 nm). The published model of the AE36s has changed wavelength 660 to 630 nm, but during the campaign a prototype version of the AE36 was utilized with the 660 nm wavelength.

The loading correction used in the AE33 and AE36 models is the dualspot correction described in Drinovec et al. (2015) and the default C_{ref} value is 1.39 when using the default M8060 filter type.

The default C_{ref} value has been observed to be underestimated causing an overestimation of the σ_{abs} and *eBC* concentrations, when compared to a multi angle absorption photometer (MAAP) (Zanatta et al., 2016; Cuesta-Mosquera et al., 2024). MAAP differs from the Aethalometer by measuring backscattering from the filter at two angles improving the accuracy of the σ_{abs} and *eBC*. MAAP is in many studies considered as a reference instrument and basis for MAC calculations due to the more advanced measurement method and high agreement with independent extinction-scattering reference methods (Petzold et al., 2005; Zanatta et al., 2016; Alas et al., 2020; T. Müller & M. Fiebig, 2021; Cuesta-Mosquera et al., 2024; Savadkoohi et al., 2024). Therefore, when calculating absorption, additional harmonization factor *H* of 1.76 is applied to the data (Eq. 5) according to the ACTRIS recommendations (T. Müller & M. Fiebig, 2021). Harmonization factors can be derived for different absorption photometers to bring all measurement devices to compliance with the reference method MAAP:

$$\sigma_{abs,harmonized} = \frac{\sigma_{abs}}{H} \quad [5]$$

2.3 Data processing and error estimation

2.3.1 Lab OC/EC error estimation

The Lab OC/EC analyzer measures the OC and EC as micrograms per square centimeter [µg C cm^{-2}] relative to the filter punch. This result is converted to mass concentration as seen in Eq. 6:

$$OC = \frac{OC_{MEAS} * A}{V}, \quad [6]$$

where *OC* is the mass concentration, OC_{MEAS} is the measurement given by the instrument, *A* is the collection area on the original filter (circle) and *V* is the volume of air pumped through the respective filter. *EC* concentration is calculated similarly, and *TC* concentration is a simple sum of the *OC* and *EC*.

The error estimation for the Lab OC/EC analyser is done with according to the EBAS submission guidelines (J. P. Putaud, 2013) as seen in Eq. 7

$$\frac{\Delta OC}{OC} = \sqrt{\frac{(OC_{\mathrm{MEAS}} * \Delta OC_{\mathrm{MEAS}})^2 + \sigma_{\mathrm{BLANK}}{}^2}{OC_{\mathrm{MEAS}}{}^2} + \left(\frac{\Delta A_p}{A_p}\right)^2 + \left(\frac{\Delta \mathrm{A}}{A}\right)^2 + \left(\frac{\Delta \mathrm{V}}{V}\right)^2}, \quad [7]$$

where the error of the mass concentration is *ΔOC*, ΔOC_{MEAS} is the uncertainty of the instrument equivalent to 0.05, σ_{BLANK} standard deviation of the fieldblanks (0.12, 0.04 and 0.12 for OC, EC and TC respectively), A_p is the area of the filter punch (rectangle), ΔA_p

is the uncertainty of the area of the filter punch, ΔA is the uncertainty of the collection area and ΔV is the uncertainty of the volume measurement. ΔA_p and ΔA are calculated with Eqs. 8 and 9 respectively:

$$\frac{\Delta A_p}{A_p} = \sqrt{\left(\frac{0.5\ \text{mm}}{10\ \text{mm}}\right)^2 + \left(\frac{0.5\ \text{mm}}{15\ \text{mm}}\right)^2}\ , \quad [8]$$

$$\frac{\Delta A}{A} = \sqrt{2 * \left(\frac{0.25\ \text{mm}}{r}\right)^2 * \pi} \quad [9]$$

2.3.2 CASS system error estimation

Estimated TC error of TCA08 is 6 % (Rigler et al., 2020). For the eBC estimated error of 100% was used based on the EBAS submission manual. The error estimation of eBC is highly complicated and one of the main research questions of this thesis and is discussed in detail later. Root sum square (RSS) was used to estimate the error of eOC as seen in Eq. 10.

$$\Delta\text{eOC}_{CASS} = \sqrt{(\Delta\text{TC}_{CASS})^2 + (\Delta\text{eBC}_{CASS})^2}, \quad [10]$$

where ΔeOC_{CASS}, ΔTC_{CASS}, and ΔeBC_{CASS} are respective errors of eOC, TC and eBC.

2.3.3 Aethalometer scattering correction

To correct the scattering error of the Aethalometer σ_{scat} measured with a TSI 3563 Integrating Nephelometer (450 nm, 550 nm, 700 nm) was used. A nephelometer is an instrument used to measure the σ_{scat} and σ_{bscat} from aerosol particles. The instrument design and working principle of a nephelometer is described in Anderson et al. (1996) and Müller et al. (2011).

The measured σ_{scat} were corrected to standard temperature and pressure (STP, 273.15 K, 1013.25 hPa) conditions and adjusted to the AE36 wavelengths with a scattering Ångström exponent (SAE, Eq. 11). The SAE was calculated with the 450 nm and 700 nm measurements, and the adjustment was done with the nearest available scattering coefficient as seen in Eq. 11. 2% of the scattering coefficient ($s = 0.02$ in Eq. 3) was reduced from the absorption coefficient on all respective AE36s wavelengths.

$$SAE = -\frac{\log(\frac{\sigma_{\lambda_1,scat}}{\sigma_{\lambda_2,scat}})}{\log(\frac{\lambda_1}{\lambda_2})} \Rightarrow \sigma_{\lambda_2,scat} = (\frac{\lambda_2}{\lambda_1})^{-SAE} * \sigma_{\lambda_1,scat} \quad [11]$$

2.3.4 Data processing and tools

In total 5 out of 117 filter samples were removed due to bad filter spot shape, and high collection volume (>300 m^3). This results that 4.3% of data was removed.

Data was divided into winter (18.11.2022-05.04.2023) and summer (09.05.2023-2.10.2023) based on thermal seasons, where winter is defined when daily mean temperature is below 0 °C and summer when daily mean temperature is above 10 °C. Autumn and spring were not considered in this thesis due to the lack of data points.

Python3 was used for data analysis and plotting with mainly pandas, matplotlib, seaborn and numpy packages (Hunter, 2007; Harris et al., 2020; pandas development team, 2020; Waskom, 2021). Regression and correlation were calculated using scipy.odr and scipy.stats packages (Virtanen et al., 2020).

3 Results

3.1 Annual and seasonal concentrations of carbonaceous aerosol at SMEAR II

The time series of the CASS and filter measurements can be seen in Fig. 4. The higher measurement frequency of the CASS system is shown with the 1 hour mean line. Data from the CASS system is averaged to match the collection times of the offline filters shown with the dashed lines. With the higher time resolution, it is evident that the CASS system better captures the temporal variability of eOC, eBC and TC in comparison to the filter measurements. When comparing the averaged data, the CASS system measures higher concentrations by an approximate factor of 1.5 for eOC-to-OC and TC. And a factor of 3 for the eBC-to-EC.

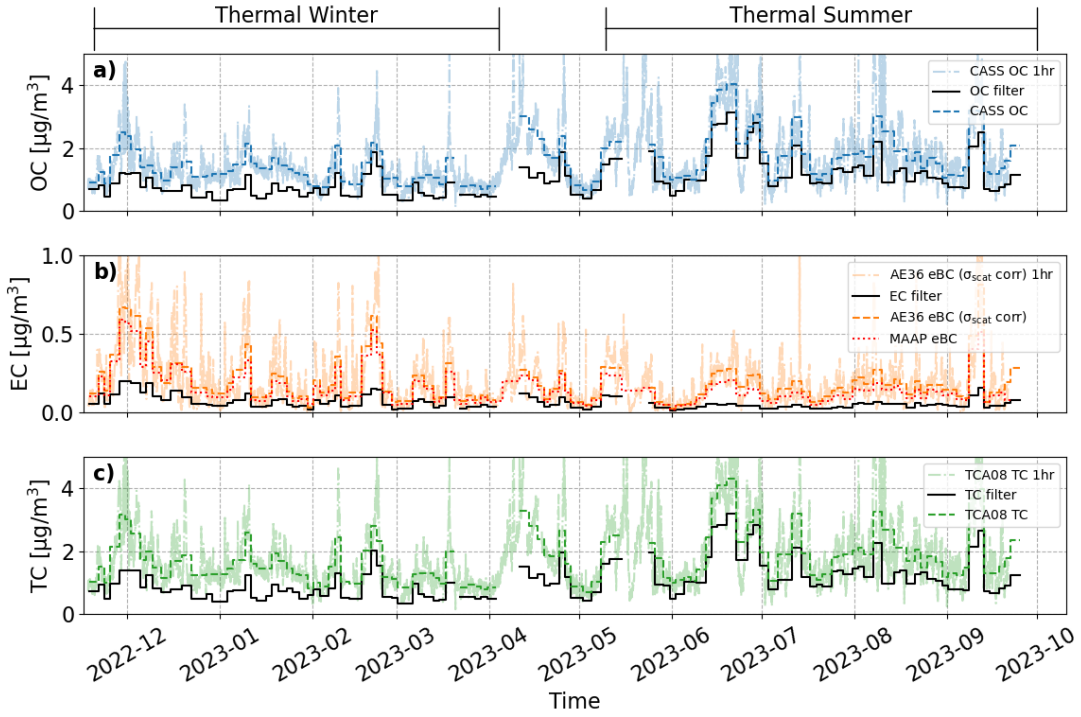


*Figure 4. Time series of **a)** OC, **b)** EC and eBC, **c)** TC in Hyytiälä in 2023. In all panels black line shows the filter measurement, dashed line the averaged CASS and MAAP measurement and opaque dashed line the 1 hour mean CASS measurement.*

The annual, winter and summer averages are shown in Table 1. The annual average concentration of OC from the filters was 1.02 ± 0.58 µg m^{-3} and from the CASS system 1.60 ± 0.70 µg m^{-3}. The filters agree well with previous publications by Aurela et al.

(2011) reporting average OC concentration of 1.1 ± 0.9 μg m^{-3} using same methodology of filter collection from Hyytiälä between 14/02/2007–18/02/2008. In seasonal comparison summertime OC concentrations remained similar (1.3 ± 0.7 μg m^{-3}, 1.2 ± 0.7 μg m^{-3} in Aurela et al. (2011)) but there was a reduction by almost half in the wintertime OC concentration from 1.3 ± 1.2 μg m^{-3} to 0.71 ± 0.31 μg m^{-3}. This is most likely due to just an overall reduction of aerosol emission from stricter regulations. This is also backed by reduction of EC concentrations with annual concentrations lowering from 0.18 ± 0.19 μg m^{-3} in 2007 to 0.06 ± 0.04 μg m^{-3} in 2023, with summer concentrations going from 0.10 ± 0.06 μg m^{-3} to 0.05 ± 0.03 μg m^{-3} and winter concentrations from 0.24 ± 0.19 μg m^{-3} to 0.08 ± 0.05 μg m^{-3} respectively. These observations are in line with other studies that have reported decreasing trends in aerosol number and volume concentration, absorption/eBC and scattering in Hyytiälä and Northern Europe (Pandolfi et al., 2018; Luoma et al., 2019; Friman et al., 2023; Savadkoohi et al., 2023; Banerji et al., 2025). It is to be noted that this reduction is limited to anthropogenic emissions as seen in the overall reduction of EC and wintertime OC. Summertime OC remaining at similar level than over a decade shows that the natural emissions from the forest have been constant.

Table 1. Annual and seasonal minimum, maximum and mean OC, eBC, EC and TC concentrations with filter and CASS measurements. All units are in μg m^{-3}.

Season	Param.	OC_{filter}	eOC_{CASS}	EC_{filter}	eBC_{CASS}	TC_{filter}	TC_{CASS}
Annual	Min-Max	0.33-3.14	0.66-4.04	0.02-0.20	0.03-0.81	0.35-3.19	0.71-4.32
	Mean ±STD	1.02 ± 0.58	1.60 ± 0.70	0.06 ± 0.04	0.20 ± 0.14	1.09 ± 0.60	1.79 ± 0.79
Winter	Min-Max	0.33-1.86	0.70-2.51	0.02-0.20	0.03-0.67	0.35-2.02	0.81-3.18
	Mean ±STD	0.71 ± 0.31	1.29 ± 0.45	0.08 ± 0.05	0.23 ± 0.17	0.79 ± 0.35	1.52 ± 0.60
Summer	Min-Max	0.48-3.14	0.98-4.04	0.02-0.15	0.03-0.81	0.49-3.19	1.01-4.32
	Mean ±STD	1.34 ± 0.65	1.87 ± 0.78	0.05 ± 0.03	0.18 ± 0.12	1.39 ± 0.66	2.05 ± 0.86

3.2 Correlation between filter and CASS measurements

The two measurement methods showed a good annual Pearson correlation r^2 of ~0.9 ($p << 0.05$ on all correlations r^2) as shown in Table 2 and Fig. 5. With the higher concentrations from the CASS system the slope of eOC-to-OC and TC were 1.49 ± 0.03 and 1.60 ± 0.06 respectively. eBC-to-EC showed a higher slope of 3.31 ± 0.07. The differences in TC and eOC-to-OC are most likely due to the negative sampling artifact of volatilization and mechanical forces from longer collection time, time between analysis and handling of the filter causing losses on the traditional filter samples (Rigler et al., 2020). This can be seen in Fig. 6, as the average difference between the traditional filter and CASS system seems to increase with larger collection volume and longer collection times. Also, positive artifact of VOC adsorption is most pronounced at the 1 h sampling time for the CASS system which was used during the measurements (Gregoric et al., 2020; Rigler et al., 2020). This could account for the remaining difference especially in environment like Hyytiälä where the forest emits significant BVOCs (Yli-Juuti et al., 2021; Hakola et al., 2023). Similar positive artifacts are not expected with traditional filters as the VOC gases can evaporate overtime and the filters were analyzed several months after collection.

The larger difference between eBC-to-EC can be due to variety of reasons. This is affected by the negative sampling artifacts on the traditional filters but more importantly due to enhanced absorption in the optical measurement of the Aethalometer. The absorption of BC particles can be increased due to coating and mixing effects with clear non-absorbing particles, where there is a high ratio between non-BC to BC mass concentration (Lack & Cappa, 2010; Liu et al., 2017; Cappa et al., 2019). The enhanced absorption has been previously reported to be small in near-source environments (Cappa et al., 2019), but high with wood or biomass burning sources or with strong aging and mixing (Liu et al., 2017; Zhang et al., 2018) both in laboratory and ambient measurements. The aethalometer does not take into account enhanced absorption in the assumption of static MAC.

In a remote environment like Hyytiälä the coating of BC can be assumed to be highly likely as there is an abundance of organic precursors and particles due to the boreal forest (Jimenez et al., 2009; Jokinen et al., 2022). Also, the local and regional sources of BC are mainly wood or biomass burning (ymparisto.fi, 2026) forming already mixed and coated

BC particles or the BC particles are well aged due to long travel distance in the atmosphere. There are no significant local sources of BC emissions as the traffic rates in the region are low compared to urban environments.

Ivančič et al. (2022) achieved similar correlation (r^2 ~0.9) but better slopes (~1.1) in an urban environment of Los Angeles when using a DRI instrument (Chen et al., 2015) with TOR-method and IMPROVE_A thermal protocol as reference. As discussed in 2.1.1.1 TOT and TOR corrections can have a significant difference of 30% (TOT < TOR for EC) with the same thermal protocol. The use of different thermal protocols can additionally have a significant difference of up to ~100 % (Bai et al., 2018). Further studies with aim of harmonizing OC/EC studies could be valuable.

Table 2. Correlation parameters

Season	Param	OC	BC/EC (AE36)	BC/EC (MAAP)	TC
Annual	Slope	1.49±0.03	3.31±0.07	2.67±0.04	1.60±0.06
	Correlation r^2	0.90	0.93	0.96	0.90
Winter	Slope	1.78±0.06	3.11±0.07	2.65±0.05	1.91±0.05
	Correlation r^2	0.81	0.98	0.98	0.87
Summer	Slope	1.36±0.03	3.97±0.15	2.86±0.09	1.45±0.03
	Correlation r^2	0.93	0.91	0.93	0.93

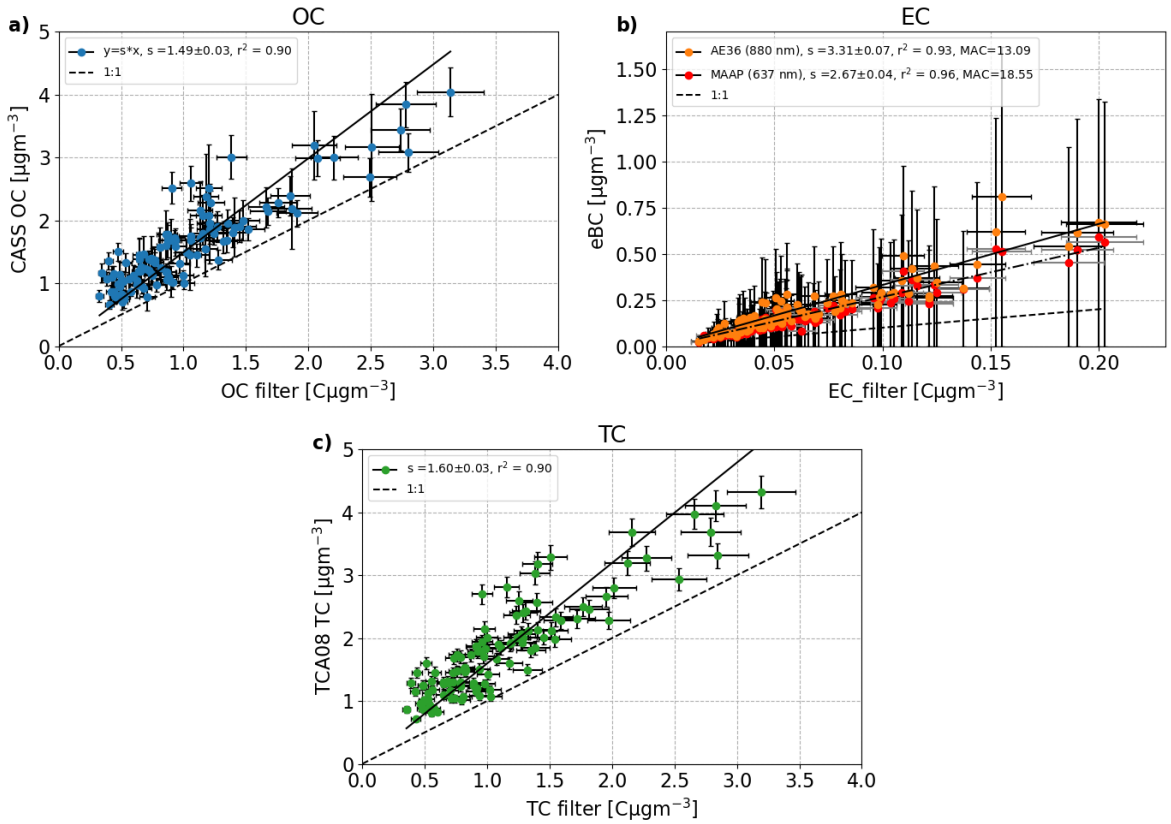


*Figure 5. Correlation r^2 between CASS and filter measurements of **a)** TC, **b**) OC, **c)** EC with AE36 880 nm and EC with MAAP 637 nm.*

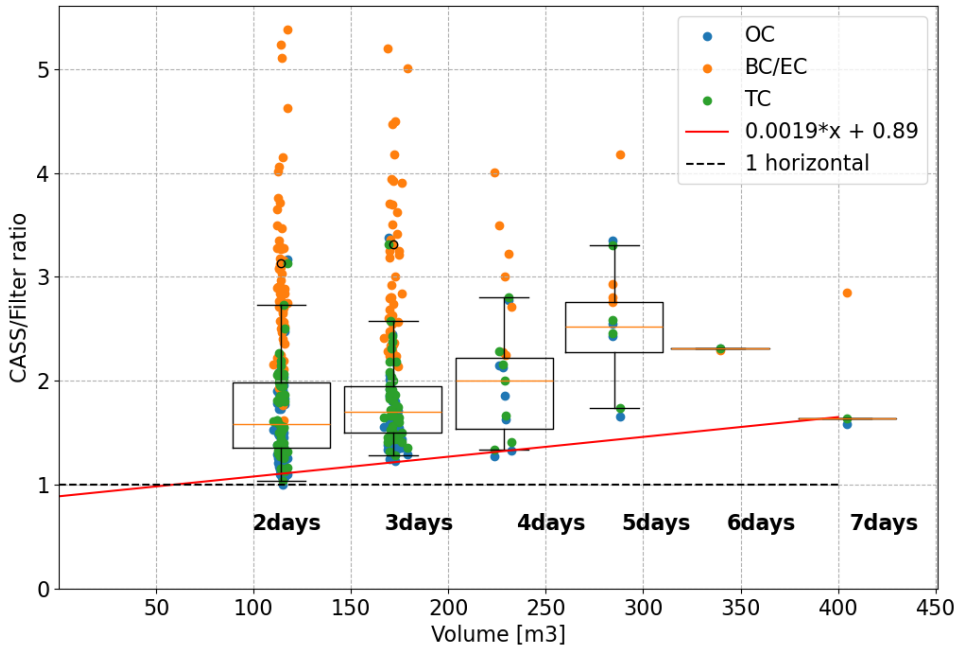


Figure 6. Ratio between CASS and filter measurements in relation to the collection volume of the filter measurements.

3.3 Seasonal correlation between filter and CASS measurements

The seasonal correlation r^2 and slope between the filters and the CASS system follows the concentration as seen in Figs. 4 and 7 and Table 2. OC and TC had lower concentrations during winter in comparison to summer and therefore slightly lower correlation r^2 of 0.81 and 0.87 with higher slopes of 1.78 ± 0.06 and 1.91 ± 0.05, respectively. The corresponding summer values were 0.93 and 0.93 with slopes of 1.36 ± 0.03 and 1.45 ± 0.03. With eBC and EC the opposite is true with higher concentrations during winter giving correlation r^2 of 0.98 and slope of 3.11 ± 0.07 with summer values being 0.91 and 3.97 ± 0.15.

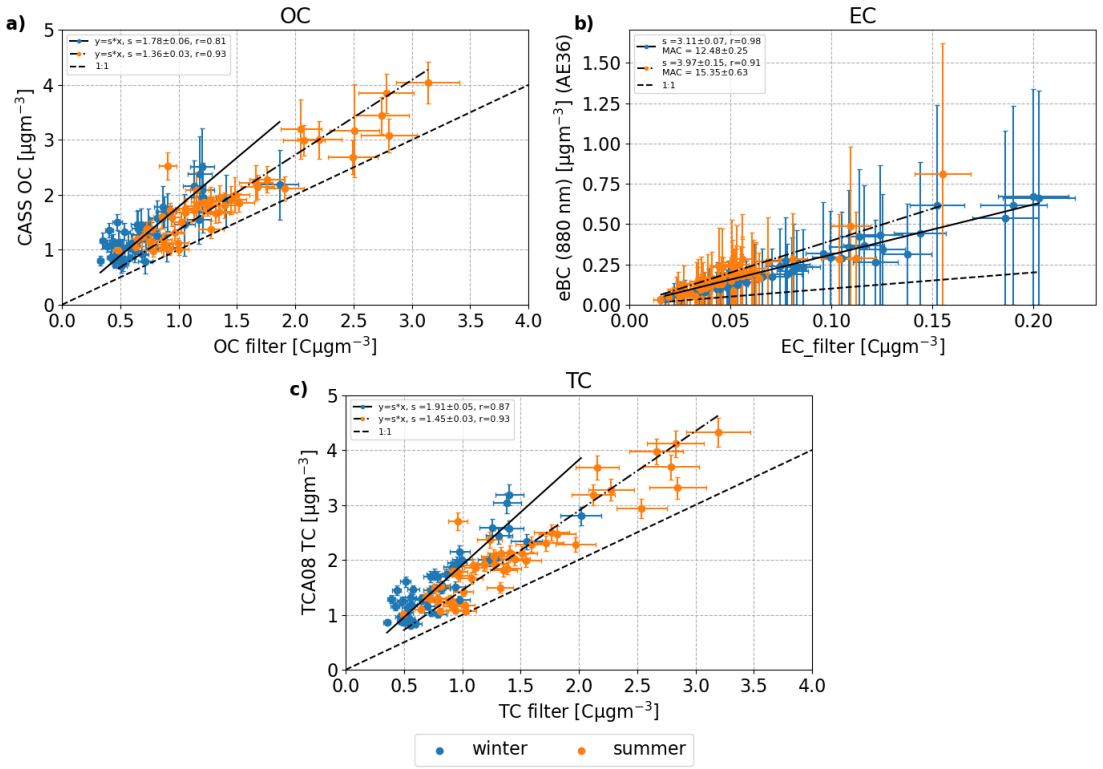


*Figure 7. Correlation r^2 between the methods of **a)** OC, **b)** EC and **c)** TC during winter and summer in Hyytiälä 2023.*

Ratios of eOC-to-OC, eBC-to-EC and TC between the measurement systems are shown in Fig. 8. The lowest ratio for eOC-to-OC and TC is observed in June and July and the highest during January. Negative artifact reduces the traditional filter concentrations and positive artifacts of VOC adsorption should be low with both the CASS system and traditional filters during winter. With higher summer concentrations the percentage error of the negative sampling artifacts with the traditional filters should be less. Positive artifacts from VOC adsorption are higher but it seems that the sensitivity of the TOA

method is improved during summer due to the higher concentration. Differences between the methods could be affected by the different inlet cutoffs utilized during the campaign (2.5 µm CASS, 10 µm traditional filter). The size distribution could have a second coarse mode during summer due to, for example primary pollen and spores reducing the difference between the methods as CASS won't measure this mode. With eBC-to-EC the highest ratio is observed in June, where the emission of organics is the highest (Heikkinen et al., 2020). During July and autumn this ratio gradually reduces showing less coating and absorption enhancement that causes the overestimation of eBC-to-EC in the CASS system. During winter the ratio is relatively stable with differences following the OC and TC concentration indicating again the effect of coating.

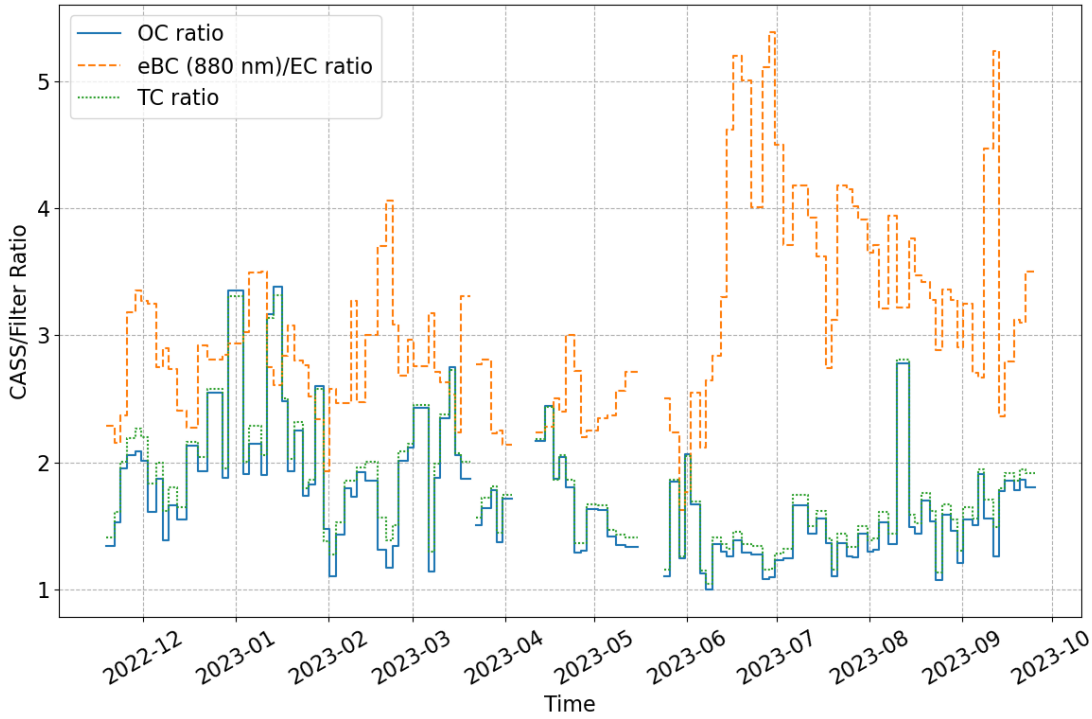


Figure 8. Ratio between CASS system and traditional filter measurements of eOC-to-OC, eBC-to-EC and TC in Hyytiälä 2023.

3.4 Ratio of organic and elemental carbon and the evolution of mass absorption cross section

Ratio between OC and EC were significantly higher in this study than in 2007 (Aurela et al., 2011) as seen in Fig. 9. In 2007 OC/EC varied from 4.8 to 13 whereas in this study the ratio varied between 4.7 to 63.0. This is due to the reduction of EC concentration over the last decade. The seasonal variation was similar with gradual rise during spring, peak

in June and gradual decrease in autumn. The correlation r^2 between OC and EC was slightly lower in winter as seen in Fig. 10 (0.81, 0.92-0.94 in Aurela et al. (2011)) and significantly lower in summer (0.47, 0.74 in Aurela et al. (2011)). These observations indicate the reduction of combustion and that carbon concentration of the aerosol particles is dominated with secondary biogenic aerosol formation even more than in 2007. The sources and concentrations of EC have reduced and are mainly transported from long distances. Also, low correlation r^2 shows that OC and EC are not produced by the same source.

Ratio between eOC and eBC was not as high as OC and EC due to the overestimation of eBC from the absorption enhancement but showed similar seasonal variation pattern as OC and EC ratio.

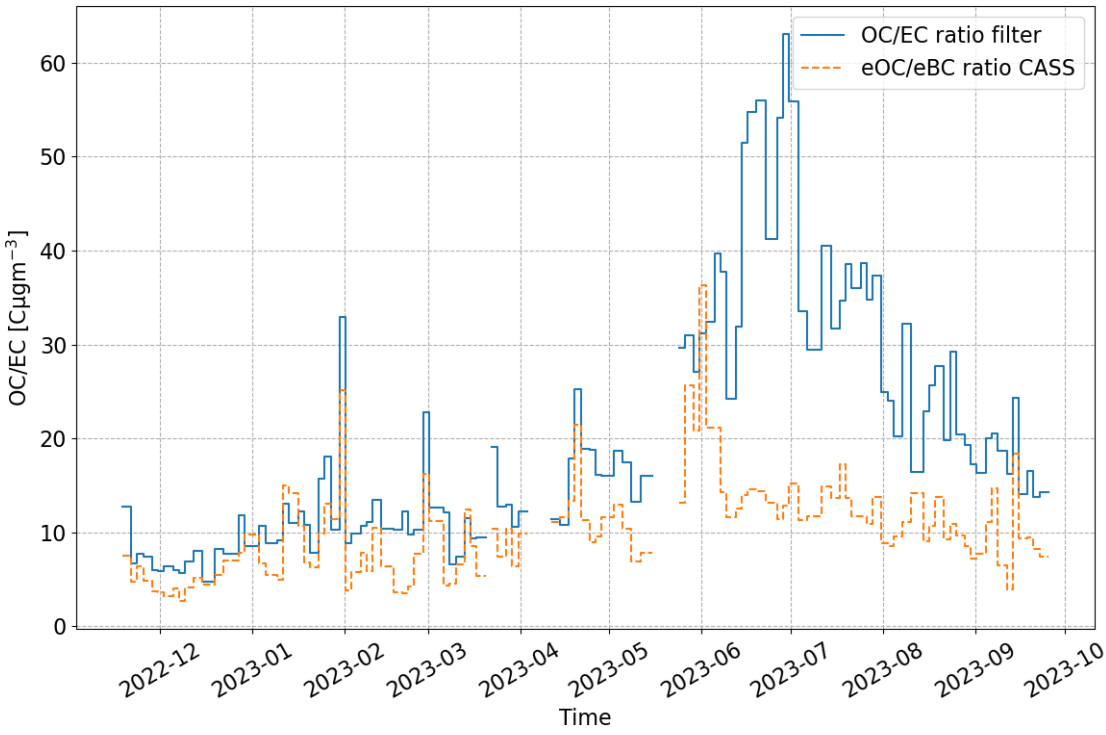


Figure 9. OC/EC ratio from the offline filter measurements and eOC/eBC ratio from the CASS measurements.

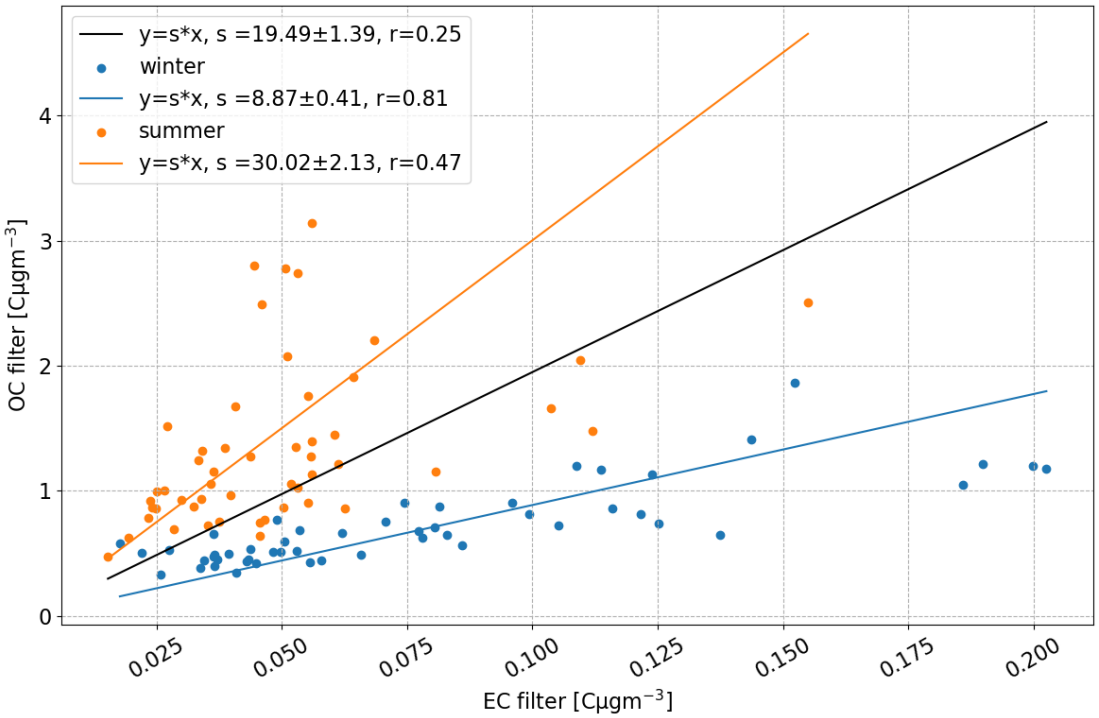


Figure 10. Correlation r^2 between OC and EC for thermal winter and summer. The black line represents both seasons.

The mean MAC for MAAP in Hyytiälä was significantly higher (16.86 ± 3.26 m^2 g^{-1}), than previously reported (7.3 ± 4.7 m^2 g^{-1}) by Savadkoohi et al. (2024) as seen in Fig. 11. The same calculation for the absorption was used but for the measurement of EC Savadkoohi et al. (2024) used data from an online instrument. The working principle of the online instrument is the same TOA, but the reason for such large difference is not clear. Asmi et al. (2025) reported variable global MACs ranging from 2.6 – 26.6 m^2 g^{-1} with a remote station average of 12.8 m^2 g^{-1}. With AE36 the recommended MAC at 880 nm is 7.8 ± 3.4 m^2 g^{-1} (Savadkoohi et al., 2024). MAC of 11.69 ± 2.88 m^2 g^{-1} was calculated in this study with the scattering correction which is not taken into account in the recommendations. Without the scattering correction the MAC was significantly higher 23.74 ± 5.94 m^2 g^{-1}. For AE36 at 660 nm and with the scattering correction a MAC of 16.47 ± 3.67 m^2 g^{-1} was calculated which close to the MAAP. Without scattering correction, the MAC was high 34.29 ± 8.37 m^2 g^{-1}. This illustrates the importance of scattering correction as it can significantly affect the estimation of eBC concentration.

The higher MAC is expected in Hyytiälä due to the remote environment as mentioned in Sect. 3.2. This would suggest significant coating and absorption enhancement for the

absorbing aerosol in Hyytiälä. Significant seasonal variability in the MAC can also be observed in Fig. 11. This shows that the aerosol particles can be very dynamic in short timespans and the presumption of constat MAC is insufficient at sites like Hyytiälä. This error affects the CASS system that is reliant on the MAC for the accurate description of the optical-thermal relationship between eBC and EC in order to determine both eOC and eBC. With long-term measurements the changing trend of the MAC requires regular re-evaluation of the eBC-to-EC optical-thermal relationship. This causes that the new CASS system can be used to increase the observational data coverage, but it can't fully replace the TOA measurement method.

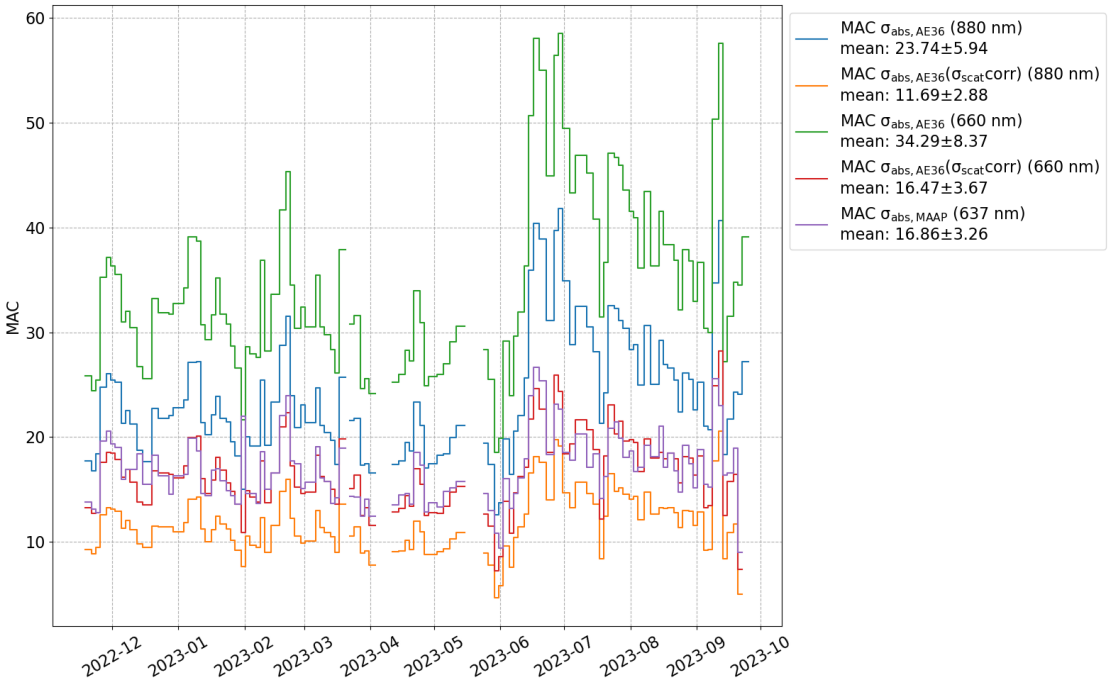


Figure 11. Timeseries of MAC derived from different absorption measurements (AE36 and MAAP).

4 Conclusions

In this study eOC-OC, eBC-EC and TC measurements were conducted with Carbonaceous Aerosol Speciation System (CASS) and traditional filter measurements to compare and validate the comparability of the measurement methods and acquire information about carbon concentrations in the atmosphere.

When compared to previous study (Aurela et al., 2011), the overall concentration of eBC-EC and wintertime OC has reduced significantly over the past decade due to reduction in combustion. The summertime OC concentration has remained similar. The source of OC is even more dominated by local biogenic particle emission and formation because the transport of long-range emissions has reduced. eBC-EC is predominantly coming from long-range transport and therefore has also reduced. eBC-EC is significantly aged and coated based on the overestimation of eBC due to absorption enhancement.

The CASS system showed to be more sensitive to concentrations of TC as the traditional filter samples suffered from higher losses. This was due to negative artifacts caused by volatilization and mechanical forces from longer collection time, time between analysis and handling of the filter. The positive artifact of VOC adsorption raised CASS system concentrations adding to the difference between the methods. The CASS system showed the benefits of a higher time resolution (20 min < 2-7 days) being able to better capture the temporal variability of TC, eOC and eBC.

With the eBC-EC comparison and the determination of the eOC in the CASS system the multiple scattering, aerosol scattering and loading effect corrections of the Aethalometer need to be considered. This causes several issues and failure points in the comparison of the optical-thermal relationship between eBC-EC. The accurate determination of MAC is essential to give an accurate estimation of eBC and eOC in the CASS system, therefore the full replacement of the traditional filter collection and thermal analysis may not be possible without additional studies to the relationship between particle mass, composition and optical properties. Consistently in the results the eOC is underestimated, and eBC is overestimated in the CASS system when deployed in Hyytiälä. Significant seasonal variation of the MAC was also observed. It is to be noted that in the traditional thermal-optical analysis different results can be obtained with different thermal protocols and

optical correction methods during the analysis. Therefore, inherently the fractions of OC and EC have some definitional uncertainty and further comparisons between the CASS and other thermal protocols, and optical corrections should be conducted.

5 References

Alas, H. D. C., Müller, T., Weinhold, K., Pfeifer, S., Glojek, K., Gregorič, A., Močnik, G., Drinovec, L., Costabile, F., Ristorini, M., & Wiedensohler, A. (2020). Performance of microaethalometers: Real-world field intercomparisons from multiple mobile measurement campaigns in different atmospheric environments. *Aerosol and Air Quality Research*, *20*(12). https://doi.org/10.4209/aaqr.2020.03.0113

Anderson, T. L., Covert, D. S., Marshall, S. F., Laucks, M. L., Charlson, R. J., Waggoner, A. P., Ogren, J. A., Caldow, R., Holm, R. L., Quant, F. R., Sem, G. J., Wiedensohler, A., Ahlquist, N. A., & Bates, T. S. (1996). Performance characteristics of a high-sensitivity, three-wavelength, total scatter/backscatter nephelometer. *Journal of Atmospheric and Oceanic Technology*, *13*(5). https://doi.org/10.1175/1520-0426(1996)013<0967:PCOAHS>2.0.CO;2

Asmi, E., Sipkens, T. A., Saturno, J., Backman, J., Vasilatou, K., Weingartner, E., Keller, A., Ciupek, K., Müller, T., Babu Suja, A., Močnik, G., Drinovec, L., Eleftheriadis, K., Gini, M. I., Nowak, A., & Corbin, J. C. (2025). Mass absorption cross-section of ambient black carbon aerosols - a review. *Npj Climate and Atmospheric Science*, *9*(1). https://doi.org/10.1038/s41612-025-01288-2

Aurela, M., Saarikoski, S., Timonen, H., Aalto, P., Keronen, P., Saarnio, K., Teinilä, K., Kulmala, M., & Hillamo, R. (2011). Carbonaceous aerosol at a forested and an urban background sites in Southern Finland. *Atmospheric Environment*, *45*(7). https://doi.org/10.1016/j.atmosenv.2010.12.039

Banerji, S., Luoma, K., Ylivinkka, I., Ahonen, L., Kerminen, V. M., & Petäjä, T. (2025). Measurement report: Optical properties of supermicron aerosol particles in a boreal environment. *Atmospheric Chemistry and Physics*, *25*(22). https://doi.org/10.5194/acp-25-16895-2025

Bautista, A. T., Pabroa, P. C. B., Santos, F. L., Quirit, L. L., Asis, J. L. B., Dy, M. A. K., & Martinez, J. P. G. (2015). Intercomparison between NIOSH, IMPROVE_A, and EUSAAR_2 protocols: Finding an optimal thermal-optical protocol for Philippines OC/EC samples. *Atmospheric Pollution Research*, *6*(2). https://doi.org/10.5094/APR.2015.037

Birch, M. E., & Cary, R. A. (1996). Elemental Carbon-Based Method for Monitoring Occupational Exposures to Particulate Diesel Exhaust. *Aerosol Science and Technology*, *25*(3). https://doi.org/10.1080/02786829608965393

Cappa, C. D., Zhang, X., Russell, L. M., Collier, S., Lee, A. K. Y., Chen, C. L., Betha, R., Chen, S., Liu, J., Price, D. J., Sanchez, K. J., McMeeking, G. R., Williams, L. R., Onasch, T. B., Worsnop, D. R., Abbatt, J., & Zhang, Q. (2019). Light Absorption by Ambient Black and Brown Carbon and its Dependence on Black Carbon Coating State for Two California, USA, Cities in Winter and Summer. *Journal of Geophysical Research: Atmospheres*, *124*(3). https://doi.org/10.1029/2018JD029501

Cavalli, F., Viana, M., Yttri, K. E., Genberg, J., & Putaud, J. P. (2010). Toward a standardised thermal-optical protocol for measuring atmospheric organic and elemental carbon: The EUSAAR protocol. *Atmospheric Measurement Techniques*, *3*(1). https://doi.org/10.5194/amt-3-79-2010

Chan, T. W., Huang, L., Banwait, K., Zhang, W., Ernst, D., Wang, X., Watson, J. G., Chow, J. C., Green, M., Czimczik, C. I., Santos, G. M., Sharma, S., & Jones, K. (2019). Inter-comparison of elemental and organic carbon mass measurements from three North American national long-term monitoring networks at a co-located site. *Atmospheric Measurement Techniques*, *12*(8). https://doi.org/10.5194/amt-12-4543-2019

Chiappini, L., Verlhac, S., Aujay, R., Maenhaut, W., Putaud, J. P., Sciare, J., Jaffrezo, J. L., Liousse, C., Galy-Lacaux, C., Alleman, L. Y., Panteliadis, P., Leoz, E., & Favez, O. (2014). Clues for a standardised thermal-optical protocol for the assessment of organic and elemental carbon within ambient air particulate matter. *Atmospheric Measurement Techniques*, *7*(6). https://doi.org/10.5194/amt-7-1649-2014

Chow, J. C., Watson, J. G., Chen, L. W. A., Arnott, W. P., Moosmüller, H., & Fung, K. (2004). Equivalence of elemental carbon by thermal/optical reflectance and transmittance with different temperature protocols. *Environmental Science and Technology*, *38*(16). https://doi.org/10.1021/es034936u

Chow, J. C., Watson, J. G., Chen, L. W. A., Chang, M. C. O., Robinson, N. F., Trimble, D., & Kohl, S. (2007). The IMPROVE_A temperature protocol for thermal/optical carbon analysis: Maintaining consistency with a long-term database. *Journal of the Air and Waste Management Association*, *57*(9). https://doi.org/10.3155/1047-3289.57.9.1014

Chow, J. C., Watson, J. G., Crow, D., Lowenthal, D. H., & Merrifield, T. (2001). Comparison of IMPROVE and NIOSH Carbon Measurements. *Aerosol Science and Technology*, *34*(1). https://doi.org/10.1080/02786820119073

Cuesta-Mosquera, A., Glojek, K., Močnik, G., Drinovec, L., Gregorič, A., Rigler, M., Ogrin, M., Romshoo, B., Weinhold, K., Merkel, M., Van Pinxteren, D., Herrmann, H., Wiedensohler, A., Pöhlker, M., & Müller, T. (2024). Optical properties and simple forcing efficiency of the organic aerosols and black carbon emitted by residential wood burning in rural central Europe. *Atmospheric Chemistry and Physics*, *24*(4). https://doi.org/10.5194/acp-24-2583-2024

Drinovec, L., Močnik, G., Zotter, P., Prévôt, A. S. H., Ruckstuhl, C., Coz, E., Rupakheti, M., Sciare, J., Müller, T., Wiedensohler, A., & Hansen, A. D. A. (2015). The "dual-spot" Aethalometer: an improved measurement of aerosol black carbon with real-time loading compensation. *Atmospheric Measurement Techniques*, *8*(5), 1965–1979. https://doi.org/10.5194/amt-8-1965-2015

Friman, M., Aurela, M., Saarnio, K., Teinilä, K., Kesti, J., Harni, S. D., Saarikoski, S., Hyvärinen, A., & Timonen, H. (2023). Long-term characterization of organic and elemental carbon at three different background areas in northern Europe. *Atmospheric Environment*, *310*. https://doi.org/10.1016/j.atmosenv.2023.119953

Hari, P., & Kulmala, M. (2005). Station for Measuring Ecosystem-Atmosphere Relations (SMEAR II). In *Boreal Environment Research* (Vol. 10, Issue 5).

Harris, C. R., Millman, K. J., van der Walt, S. J., Gommers, R., Virtanen, P., Cournapeau, D., Wieser, E., Taylor, J., Berg, S., Smith, N. J., Kern, R., Picus, M., Hoyer, S., van Kerkwijk, M. H., Brett, M., Haldane, A., del Río, J. F., Wiebe, M., Peterson, P., … Oliphant, T. E. (2020). Array programming with NumPy. In *Nature* (Vol. 585, Issue 7825). https://doi.org/10.1038/s41586-020-2649-2

Heikkinen, L., Äijälä, M., Riva, M., Luoma, K., Dällenbach, K., Aalto, J., Aalto, P., Aliaga, D., Aurela, M., Keskinen, H., Makkonen, U., Rantala, P., Kulmala, M., Petäjä, T., Worsnop, D., & Ehn, M. (2020). Long-term sub-micrometer aerosol chemical composition in the boreal forest: Inter- And intra-annual variability. *Atmospheric Chemistry and Physics*, *20*(5). https://doi.org/10.5194/acp-20-3151-2020

Heiskanen, J., Brümmer, C., Buchmann, N., Calfapietra, C., Chen, H., Gielen, B., Gkritzalis, T., Hammer, S., Hartman, S., Herbst, M., Janssens, I. A., Jordan, A., Juurola, E., Karstens, U., Kasurinen, V., Kruijt, B., Lankreijer, H., Levin, I.,

Linderson, M.-L., … Kutsch, W. (2022). The Integrated Carbon Observation System in Europe. *Bulletin of the American Meteorological Society*, *103*(3), E855–E872. https://doi.org/https://doi.org/10.1175/BAMS-D-19-0364.1

Huang, L., Brook, J. R., Zhang, W., Li, S. M., Graham, L., Ernst, D., Chivulescu, A., & Lu, G. (2006). Stable isotope measurements of carbon fractions (OC/EC) in airborne particulate: A new dimension for source characterization and apportionment. *Atmospheric Environment*, *40*(15). https://doi.org/10.1016/j.atmosenv.2005.11.062

Hunter, J. D. (2007). Matplotlib: A 2D graphics environment. *Computing in Science and Engineering*, *9*(3). https://doi.org/10.1109/MCSE.2007.55

Huntzicker J. J. and Johnson, R. L. and S. J. J. and C. R. A. (1982). Analysis of Organic and Elemental Carbon in Ambient Aerosols by a Thermal-Optical Method. In R. L. Wolff George T. and Klimisch (Ed.), *Particulate Carbon: Atmospheric Life Cycle* (pp. 79–88). Springer US. https://doi.org/10.1007/978-1-4684-4154-3_6

IPCC. (2021). Climate Change 2021—The Physical Science Basis. *Chemistry International*, *43*(4). https://doi.org/10.1515/ci-2021-0407

J. P. Putaud. (2013). *EBAS Data Submission Manual, OC/EC offline*. https://ebas-submit.nilu.no/templates/EC-OC/offline

Janssen, N. A. H., Hoek, G., Simic-Lawson, M., Fischer, P., van Bree, L., Brink, H. Ten, Keuken, M., Atkinson, R. W., Ross Anderson, H., Brunekreef, B., & Cassee, F. R. (2011). Black carbon as an additional indicator of the adverse health effects of airborne particles compared with pm10 and pm2.5. In *Environmental Health Perspectives* (Vol. 119, Issue 12). https://doi.org/10.1289/ehp.1003369

Jimenez, J. L., Canagaratna, M. R., Donahue, N. M., Prevot, A. S. H., Zhang, Q., Kroll, J. H., DeCarlo, P. F., Allan, J. D., Coe, H., Ng, N. L., Aiken, A. C., Docherty, K. S., Ulbrich, I. M., Grieshop, A. P., Robinson, A. L., Duplissy, J., Smith, J. D., Wilson, K. R., Lanz, V. A., … Worsnop, D. R. (2009). Evolution of organic aerosols in the atmosphere. *Science*, *326*(5959). https://doi.org/10.1126/science.1180353

Lack, D. A., & Cappa, C. D. (2010). Impact of brown and clear carbon on light absorption enhancement, single scatter albedo and absorption wavelength dependence of black carbon. *Atmospheric Chemistry and Physics*, *10*(9). https://doi.org/10.5194/acp-10-4207-2010

Lack, D. A., Moosmüller, H., McMeeking, G. R., Chakrabarty, R. K., & Baumgardner, D. (2014). Characterizing elemental, equivalent black, and refractory black carbon aerosol particles: A review of techniques, their limitations and uncertainties. In

Analytical and Bioanalytical Chemistry (Vol. 406, Issue 1). https://doi.org/10.1007/s00216-013-7402-3

Laj, P., Lund Myhre, C., Riffault, V., Amiridis, V., Fuchs, H., Eleftheriadis, K., Petäjä, T., Salameh, T., Kivekäs, N., Juurola, E., Saponaro, G., Philippin, S., Cornacchia, C., Alados Arboledas, L., Baars, H., Claude, A., De Mazière, M., Dils, B., Dufresne, M., … Vana, M. (2024). Aerosol, Clouds and Trace Gases Research Infrastructure (ACTRIS): The European Research Infrastructure Supporting Atmospheric Science. *Bulletin of the American Meteorological Society*, *105*(7), E1098–E1136. https://doi.org/https://doi.org/10.1175/BAMS-D-23-0064.1

Liu, D., Whitehead, J., Alfarra, M. R., Reyes-Villegas, E., Spracklen, D. V., Reddington, C. L., Kong, S., Williams, P. I., Ting, Y. C., Haslett, S., Taylor, J. W., Flynn, M. J., Morgan, W. T., McFiggans, G., Coe, H., & Allan, J. D. (2017). Black-carbon absorption enhancement in the atmosphere determined by particle mixing state. *Nature Geoscience*, *10*(3). https://doi.org/10.1038/ngeo2901

Luoma, K., Virkkula, A., Aalto, P., Petäjä, T., & Kulmala, M. (2019). Over a 10-year record of aerosol optical properties at SMEAR II. *Atmospheric Chemistry and Physics*, *19*(17). https://doi.org/10.5194/acp-19-11363-2019

Magee. (2026, March). *Magee Scientific*. https://aerosolmageesci.com

Monteiro dos Santos, D. A., Brito, J. F., Godoy, J. M., & Artaxo, P. (2016). Ambient concentrations and insights on organic and elemental carbon dynamics in São Paulo, Brazil. *Atmospheric Environment*, *144*. https://doi.org/10.1016/j.atmosenv.2016.08.081

Müller, T., Laborde, M., Kassell, G., & Wiedensohler, A. (2011). Design and performance of a three-wavelength LED-based total scatter and backscatter integrating nephelometer. *Atmospheric Measurement Techniques*, *4*(6). https://doi.org/10.5194/amt-4-1291-2011

Neefjes, I., Laapas, M., Liu, Y., Médus, E., Miettunen, E., Ahonen, L., Quéléver, L., Aalto, J., Bäck, J., Kerminen, V. M., Lampilahti, J., Luoma, K., Mäki, M., Mammarella, I., Petäjä, T., Räty, M., Sarnela, N., Ylivinkka, I., Hakala, S., … Lintunen, A. (2022). 25 years of atmospheric and ecosystem measurements in a boreal forest-Seasonal variation and responses to warm and dry years. *Boreal Environment Research*, *27*.

NIOSH. (2003). NIOSH Manual of Analytical Methods (NMAM), Fourth edition. *1003: Hydrocarbons, Halogenated*, *1016*(1).

pandas development team. (2020). pandas-dev/pandas: Pandas 1.0.3. *Zenodo*. https://doi.org/10.5281/zenodo.10957263

Pandolfi, M., Alados-Arboledas, L., Alastuey, A., Andrade, M., Angelov, C., Artiñano, B., Backman, J., Baltensperger, U., Bonasoni, P., Bukowiecki, N., Collaud Coen, M., Conil, S., Coz, E., Crenn, V., Dudoitis, V., Ealo, M., Eleftheriadis, K., Favez, O., Fetfatzis, P., … Laj, P. (2018). A European aerosol phenomenology - 6: Scattering properties of atmospheric aerosol particles from 28 ACTRIS sites. *Atmospheric Chemistry and Physics*, *18*(11). https://doi.org/10.5194/acp-18-7877-2018

Petzold, A., Ogren, J. A., Fiebig, M., Laj, P., Li, S.-M., Baltensperger, U., Holzer-Popp, T., Kinne, S., Pappalardo, G., Sugimoto, N., Wehrli, C., Wiedensohler, A., & Zhang, X.-Y. (2013). Recommendations for reporting "black carbon" measurements. *Atmospheric Chemistry and Physics*, *13*(16), 8365–8379. https://doi.org/10.5194/acp-13-8365-2013

Petzold, A., Schloesser, H., Sheridan, P. J., Arnott, W. P., Ogren, J. A., & Virkkula, A. (2005). Evaluation of multiangle absorption photometry for measuring aerosol light absorption. *Aerosol Science and Technology*, *39*(1). https://doi.org/10.1080/027868290901945

Pope, C. A., & Dockery, D. W. (2006). Health effects of fine particulate air pollution: Lines that connect. *Journal of the Air and Waste Management Association*, *56*(6). https://doi.org/10.1080/10473289.2006.10464485

Rigler, M., Drinovec, L., Lavri, G., Vlachou, A., Prevot, A. S. H., Luc Jaffrezo, J., Stavroulas, I., Sciare, J., Burger, J., Kranjc, I., Turšič, J., D. A. Hansen, A., & Mocnik, G. (2020). The new instrument using a TC-BC (total carbon-black carbon) method for the online measurement of carbonaceous aerosols. *Atmospheric Measurement Techniques*, *13*(8). https://doi.org/10.5194/amt-13-4333-2020

Rovira, J., Savadkoohi, M., Chen, G. I., Močnik, G., Aas, W., Alados-Arboledas, L., Artiñano, B., Aurela, M., Backman, J., Banerji, S., Beddows, D., Brem, B., Chazeau, B., Coen, M. C., Colombi, C., Conil, S., Costabile, F., Coz, E., de Brito, J. F., … Pandolfi, M. (2025). A European aerosol phenomenology – 9: Light absorption properties of carbonaceous aerosol particles across surface Europe. *Environment International*, *195*, 109185. https://doi.org/https://doi.org/10.1016/j.envint.2024.109185

Savadkoohi, M., Pandolfi, M., Favez, O., Putaud, J. P., Eleftheriadis, K., Fiebig, M., Hopke, P. K., Laj, P., Wiedensohler, A., Alados-Arboledas, L., Bastian, S., Chazeau, B., María, Á. C., Colombi, C., Costabile, F., Green, D. C., Hueglin, C., Liakakou, E., Luoma, K., … Querol, X. (2024). Recommendations for reporting equivalent black carbon (eBC) mass concentrations based on long-term pan-European in-situ observations. *Environment International*, *185*. https://doi.org/10.1016/j.envint.2024.108553

Savadkoohi, M., Pandolfi, M., Reche, C., Niemi, J. V., Mooibroek, D., Titos, G., Green, D. C., Tremper, A. H., Hueglin, C., Liakakou, E., Mihalopoulos, N., Stavroulas, I., Artiñano, B., Coz, E., Alados-Arboledas, L., Beddows, D., Riffault, V., De Brito, J. F., Bastian, S., … Querol, X. (2023). The variability of mass concentrations and source apportionment analysis of equivalent black carbon across urban Europe. *Environment International*, *178*. https://doi.org/10.1016/j.envint.2023.108081

Sunset Labs. (2024). *Methodology, Sunset Labs*. Https://Www.Sunlab.Com/about-Us/Methodology/.

T. Müller, & M. Fiebig. (2021, September 14). *ACTRIS In Situ Aerosol: Guidelines for Manual QC of AE33 absorption photometer data*. CAIS-ECAC. https://www.actris-ecac.eu/particle-light-absorption.html

Virkkula, A., Chi, X., Ding, A., Shen, Y., Nie, W., Qi, X., Zheng, L., Huang, X., Xie, Y., Wang, J., Petäjä, T., & Kulmala, M. (2015). On the interpretation of the loading correction of the aethalometer. *Atmospheric Measurement Techniques*, *8*(10), 4415–4427. https://doi.org/10.5194/amt-8-4415-2015

Virtanen, P., Gommers, R., Oliphant, T. E., Haberland, M., Reddy, T., Cournapeau, D., Burovski, E., Peterson, P., Weckesser, W., Bright, J., van der Walt, S. J., Brett, M., Wilson, J., Millman, K. J., Mayorov, N., Nelson, A. R. J., Jones, E., Kern, R., Larson, E., … Vázquez-Baeza, Y. (2020). SciPy 1.0: fundamental algorithms for scientific computing in Python. *Nature Methods*, *17*(3). https://doi.org/10.1038/s41592-019-0686-2

Waskom, M. (2021). seaborn: statistical data visualization. *Journal of Open Source Software*, *6*(60). https://doi.org/10.21105/joss.03021

Watson, J. G., Chow, J. C., & Chen, L.-W. A. (2005). Summary of Organic and Elemental Carbon/Black Carbon Analysis Methods and Intercomparisons. *Aerosol and Air Quality Research*, *5*(1). https://doi.org/10.4209/aaqr.2005.06.0006

Zanatta, M., Gysel, M., Bukowiecki, N., Müller, T., Weingartner, E., Areskoug, H., Fiebig, M., Yttri, K. E., Mihalopoulos, N., Kouvarakis, G., Beddows, D., Harrison, R. M., Cavalli, F., Putaud, J. P., Spindler, G., Wiedensohler, A., Alastuey, A., Pandolfi, M., Sellegri, K., … Laj, P. (2016). A European aerosol phenomenology-5: Climatology of black carbon optical properties at 9 regional background sites across Europe. *Atmospheric Environment*, *145*. https://doi.org/10.1016/j.atmosenv.2016.09.035

Zhang, Y., Favez, O., Canonaco, F., Liu, D., Močnik, G., Amodeo, T., Sciare, J., Prévôt, A. S. H., Gros, V., & Albinet, A. (2018). Evidence of major secondary organic aerosol contribution to lensing effect black carbon absorption enhancement. *Npj Climate and Atmospheric Science*, *1*(1). https://doi.org/10.1038/s41612-018-0056-2